

Frequency analysis of the stability of asteroids in the framework of the restricted, three-body problem

Alessandra Celletti

Dipartimento di Matematica

Università di Roma Tor Vergata

Via della Ricerca Scientifica 1, I-00133 Roma (Italy)

(celletti@mat.uniroma2.it)

Claude Froeschlé

Observatoire de Nice

B.P. 229

06304 Nice Cedex 4 (France)

(claude@obs-nice.fr)

Elena Lega

Observatoire de Nice

B.P. 229

06304 Nice Cedex 4 (France)

(elena@obs-nice.fr)

October 16, 2003

Abstract

The stability of some asteroids, in the framework of the restricted three body problem, has been recently proved in [2] by developing an isoenergetic KAM theorem. More precisely, having fixed a level of energy related to the motion of the asteroid, the stability can be obtained by showing the existence of nearby trapping invariant tori living on the same energy level. The analytical results are compatible with the astronomical observations, since the theorem is valid for the realistic mass-ratio of the primaries.

The model adopted in [2] is the planar, circular, restricted three-body model, in which only the most significant contributions of the Fourier development of the perturbation are retained. In this paper we investigate numerically the stability of the same asteroids considered in [2] (namely, Iris, Victoria and Renzia). In particular, we implement the nowadays standard method of frequency-map analysis and we compare our investigation with the analytical results on the planar, circular model with the truncated perturbing function. By means of frequency analysis, we study the behaviour of the bounding tori and henceforth we infer stability properties on the dynamics of the asteroids. In order to test the validity of the truncated Hamiltonian, we consider also the complete expression of the perturbing function on which we perform again frequency analysis. We investigate also more realistic models, taking into account the eccentricity of the trajectory of Jupiter (planar-elliptic problem) or the relative inclination of the orbits (circular-inclined model). We did not find a relevant discrepancy among the different models, except for the case of Renzia, that we explain in terms of its proximity to a resonance.

Keywords: Three-body problem, Stability, Frequency analysis.

1 Introduction

The stability of some asteroids under the gravitational attraction of the Sun and Jupiter has been recently investigated in [2], where analytical results are derived in the context of the simplest non-trivial three-body problem. More specifically, one assumes that the mass of the minor body does not influence the motion of the primaries (*restricted* problem), that Jupiter moves on a circular orbit and that the relative inclination is zero. Using Hamiltonian formalism, the *planar, circular, restricted three-body problem* can be conveniently described in terms of a suitable combination of Delaunay's action-angle variables. Such model has two degrees of freedom and the Hamiltonian function describing the motion of the asteroid is nearly-integrable: the integrable part describes the Sun-asteroid Keplerian motion, while the perturbation represents the interaction with Jupiter. The perturbing parameter is identified with the mass-ratio of the primaries. A further simplification of the problem is performed in [2], where the authors expand the perturbing function in Fourier series and they retain only a finite number of terms of the series development.

Since the Hamiltonian system is 2-dimensional, invariant tori separate the constant energy levels. More precisely, the phase-space is 4-dimensional; fixing an energy level (related to the motion of the asteroid), one obtains a 3-dimensional space, in which invariant 2-dimensional tori live. Therefore, the stability of the asteroid can be ensured by constructing two invariant surfaces, which bound from below and above (on the given energy level) the motion of the minor body. Under very general assumptions, the KAM theory developed by A.N. Kolmogorov ([5]), V.I. Arnold ([1]) and J. Moser ([10]) allows to construct an explicit algorithm to ensure the existence of invariant tori, provided that the strength of the perturbation is sufficiently small. In the framework of KAM theory, a major problem was due to the fact that the estimates provided by the original theorems were unrealistically small. To give an example, M. Hénon ([4]) applied to the three-body problem the original version of Arnold's theorem and he was able to prove the existence of invariant tori, provided that the mass-ratio of the primaries is less than 10^{-333} . A better result was obtained applying Moser's theorem, which provides an estimate of 10^{-50} , whereas the astronomical value of the Jupiter-Sun mass-ratio amounts to about 10^{-3} . The disagreement between the analytical results and the physical measurements was rather discouraging, as far as *practical* applications are concerned. However, in the last two decades the development of computer-assisted proofs greatly improved the theoretical estimates, leading to results which are now much closer to reality.

In particular, in [2] an elaborated *isoenergetic* KAM theorem has been developed to investigate the motion of some asteroids in the framework of the planar, circular, restricted three-body problem, using a finite series development of the perturbing function. Such theorem has been successfully applied to the study of the stability of the asteroids Iris (n. 7), Victoria (n. 12) and Renzia (n. 1204) (the numbers denote the standard classification of the asteroidal objects, see e.g. [12]; in [2] the analytical details of the proof are given for Victoria). In all samples, it was possible to prove the existence of invariant tori bounding, from below and above, the motion of the asteroid on a fixed energy level. The theorem is valid provided the perturbing parameter is less than 10^{-3} , in full agreement with the astronomical observations of the Jupiter-Sun mass-ratio.

In the present paper we complement the results of [2] by providing a numerical inspection of the stability of the asteroids Iris, Victoria and Renzia. The problem is investigated by implementing the frequency analysis, as introduced by J. Laskar in [7], [8]. In order to test the

validity of the model adopted in [2], we perform our experiments on different models. Indeed, in the framework of the planar, circular, restricted three-body problem, we compare the models obtained using the truncated Hamiltonian (i.e. retaining a finite number of Fourier terms as in [2]) and the complete Hamiltonian (i.e. without any truncation of the perturbing function). The results show that the truncated model provides a good approximation of the full Hamiltonian. Furthermore, we release the hypothesis of circular orbit by assuming that Jupiter moves on a Keplerian elliptic trajectory, but we retain the assumption that the motion of the three bodies takes place on the same plane. We still consider only a finite number of Fourier coefficients; in the cases of Iris and Victoria, the results show a good agreement with the circular problem, in the sense that there is no remarkable discrepancy between the critical values of the perturbing parameter at which break-down of invariant tori takes place. A more evident discrepancy is found in the analysis of Renzia, whose frequency of motion is close to an exact $7/2$ orbital resonance; in this case, the planar, circular model hides the effect of the resonance, since it does not contain a number of Fourier harmonics adequate to the analysis of quasi-resonant $7/2$ motions.

Finally, we investigate a model in which Jupiter still describes a circular trajectory, but the orbits of the asteroid and Jupiter belong to different planes with non-zero relative inclination. The Fourier development of the Hamiltonian is truncated up to a suitable order. The results are compared to the previous models and, in the cases of Iris and Victoria, there is a good agreement with the planar-circular and planar-elliptic, restricted three-body models.

This paper is organized as follows. In section 2 we introduce the different restricted three-body models: planar-circular (providing also the formulae for the integration of the full perturbing function and for the development in Fourier series), planar-elliptic, inclined-circular. The principles of the implementation of frequency analysis are recalled in section 3. The results are presented in section 4, while the conclusions are drawn in section 5.

2 The restricted three-body problem

We consider three massive bodies P_0 , P_1 and P_2 with masses m_0 , m_1 and m_2 . In applications, we shall identify P_0 with the Sun, P_1 with an asteroid and P_2 with Jupiter. Therefore, a reasonable simplification consists in assuming that m_1 is much smaller than m_0 and m_2 ; as a consequence, we can assume that P_1 does not influence gravitationally the motion of the *primaries* P_0 and P_2 . This model is widely known as the *restricted* three-body problem. In particular, we can assume that the motion of P_2 around P_0 is Keplerian: according to the value of the eccentricity of P_2 , we speak of *circular* or *elliptic* problem. Moreover, we can further simplify the model assuming that the three bodies move on the same plane: in this case, we speak of *planar* problem, while we define the *inclined* model, whenever the relative inclination between P_1 and P_2 is different from zero.

We shall provide the Hamiltonian function describing the different models (planar-circular, planar-elliptic, inclined-circular). In all cases, the Hamiltonian function is *nearly-integrable*, being a small perturbation of the Keplerian two-body problem, occurring whenever the gravitational attraction of P_2 on P_1 is neglected. The perturbing function represents the interaction

between P_1 and P_2 and the perturbing parameter is related to the mass–ratio of the primaries. In the following section, we describe the *planar, circular, restricted three–body problem*, without making any restriction on the perturbing function. In particular, we provide explicit formulae for the integration of the equations of motion. As a second step, we expand the perturbing function in Fourier series and we retain only the most significant terms of the series expansion: we refer to this model as the *truncated, planar, circular, restricted three–body problem*. Furthermore, in the context of the truncated problem, we consider the effect of the eccentricity of P_2 (*elliptic problem*) and of the relative inclination of the orbits of P_1 and P_2 (*inclined problem*).

2.1 The planar, circular problem: the full Hamiltonian function

We introduce the Hamiltonian function describing the planar, circular, restricted three–body problem by adopting a suitable set of action–angle coordinates, known as *Delaunay’s variables*: $\Lambda, \Gamma, \lambda, \gamma$ (being (Λ, λ) and (Γ, γ) conjugated variables). Let a be the major semiaxis of the osculating Keplerian orbit of P_1 and let e be its eccentricity. We assume suitable normalizations for the units of measure (see [2] for details): let $m_0 + m_2 = 1$, $\mu \equiv \frac{1}{m_0^{2/3}}$, $\varepsilon \equiv \mu m_2$. Then, the action variables are related to the elliptic elements by

$$\Lambda = \mu \sqrt{m_0 a} , \quad \Gamma = \Lambda \sqrt{1 - e^2} .$$

Concerning the angle variables, λ represents the so–called *mean anomaly*, while γ is the *argument of perihelion* (namely, the angle between the perihelion line and a reference line). Moreover, let ψ be the *longitude* of P_2 ; normalizing to one the frequency of P_2 , ψ can be identified with the time. Finally, let Ψ be the action variable conjugated to ψ .

Let (r, φ) be the instantaneous polar coordinates of P_1 and let us normalize to unity the distance between P_0 and P_2 ; then, the Hamiltonian function is given by

$$H(\Lambda, \Gamma, \Psi, \lambda, \gamma, \psi) = -\frac{1}{2\Lambda^2} + \Psi + \varepsilon R_0(\Lambda, \Gamma, \lambda, \gamma, \psi) ,$$

with

$$R_0(\Lambda, \Gamma, \lambda, \gamma, \psi) = r \cos(\varphi - \psi) - \frac{1}{\sqrt{1 + r^2 - 2r \cos(\varphi - \psi)}} ,$$

where r and φ must be expressed in terms of the canonical coordinates. Introducing the variable $\alpha \equiv \varphi - \gamma$, the perturbing function R_0 depends on the quantity $\varphi - \psi = \alpha + \gamma - \psi$. Let us perform the symplectic change of variables $(\Lambda, \Gamma, \Psi, \lambda, \gamma, \psi) \rightarrow (L, G, T, \ell, g, t)$ described by:

$$\begin{aligned} \ell &= \lambda & L &= \Lambda , \\ g &= \gamma - \psi & G &= \Gamma , \\ t &= \psi & T &= \Gamma + \Psi . \end{aligned} \tag{1}$$

The corresponding two–degrees–of–freedom Hamiltonian function reads as

$$H(L, G, \ell, g) = -\frac{1}{2L^2} - G + \varepsilon R(L, G, \ell, g) , \tag{2}$$

with

$$R(L, G, \ell, g) = r \cos(\alpha + g) - \frac{1}{\sqrt{1 + r^2 - 2r \cos(\alpha + g)}} , \tag{3}$$

where α must be expressed in terms of the Delaunay's variables. The eccentricity is provided by $e = \sqrt{1 - \frac{G^2}{L^2}}$. The equations of motion can be written as

$$\begin{aligned}\dot{\ell} &= \frac{1}{L^3} + \varepsilon [R_r r_L + R_\alpha \alpha_L] \\ \dot{g} &= -1 + \varepsilon [R_r r_G + R_\alpha \alpha_G] \\ \dot{\ell} &= -\varepsilon [R_r r_\ell + R_\alpha \alpha_\ell] \\ \dot{G} &= -\varepsilon [R_r r_g + R_\alpha \alpha_g + R_g],\end{aligned}$$

where the subscripts denote derivatives: for example, $R_r \equiv \frac{\partial R}{\partial r}$, $r_L \equiv \frac{\partial r}{\partial L}$. The computation of the derivatives of R with respect to r and α is straightforward; concerning the derivatives of r and α with respect to the Delaunay's variables, we proceed as follows. We express the instantaneous orbital radius as

$$r = \frac{a(1 - e^2)}{1 + e \cos(\varphi - \gamma)} = \frac{a(1 - e^2)}{1 + e \cos \alpha}. \quad (4)$$

Moreover, from standard Kepler's relations we have:

$$\tan \frac{\varphi - \gamma}{2} = \sqrt{\frac{1 + e}{1 - e}} \tan \frac{\nu}{2}, \quad (5)$$

where ν denotes the *eccentric anomaly* (see, e.g., [11]). Since $\alpha = \varphi - \gamma$, we find

$$\alpha = 2 \arctan \left(\sqrt{\frac{1 + e}{1 - e}} \tan \frac{\nu}{2} \right),$$

where ν can be expressed in terms of the Delaunay's variables through Kepler's equation

$$\ell = \nu - e \sin \nu.$$

In order to compute the expressions of ν , α , r in terms of the Delaunay's variables, we start by inverting Kepler's equation, so to find ν as a function of ℓ , L , G (recall that $e = \sqrt{1 - \frac{G^2}{L^2}}$). Then, we need to compute α and its derivatives, as well as r and its derivatives. To perform this task, we invert Kepler's equation using Bessel's functions according to the formula

$$\nu = \ell + e \sum_{p=1}^{\infty} \frac{1}{p} [J_{p-1}(pe) + J_{p+1}(pe)] \sin(p\ell), \quad (6)$$

where the Bessel's function of order k and generic argument x is defined by

$$J_k(x) \equiv \frac{1}{2\pi} \int_0^{2\pi} \cos(kt - x \sin t) dt.$$

The functions $J_k(x)$ can be developed in series ([6]) as

$$\begin{aligned}J_0(x) &= \sum_{n=0}^{\infty} \frac{(-1)^n}{(n!)^2} \left(\frac{x}{2}\right)^{2n} \\ J_k(x) &= \left(\frac{x}{2}\right)^k \frac{1}{k!} \sum_{n=0}^{\infty} \frac{(-1)^n}{n! \prod_{j=1}^n (k+j)} \left(\frac{x}{2}\right)^{2n}.\end{aligned} \quad (7)$$

Equations (6) and (7) can be used to find ν with arbitrary precision. Once the eccentric anomaly is determined, we can compute α using the equation

$$\alpha = 2 \arctan(f \cdot h) ,$$

where we define $f \equiv \sqrt{\frac{1+e}{1-e}}$ and $h \equiv \tan \frac{\nu}{2}$. This procedure allows to compute easily the derivatives of α ; for example, one has

$$\alpha_L = \frac{2}{1 + f^2 h^2} (f_L h + f h_L) ,$$

where the computation of f_L is straightforward (recall that $e = e(L, G)$), $h_L = \frac{1}{2 \cos^2 \frac{\nu}{2}} \nu_L$ and ν_L can be computed from (6), up to arbitrary precision. In a similar way, one computes the other derivatives.

Concerning r , from (4) we find

$$r = \frac{G^2}{1 + e \cos \alpha} \equiv \frac{\tilde{f}}{\tilde{h}} ,$$

where we define $\tilde{f} = G^2$ and $\tilde{h} = 1 + e \cos \alpha$. Simple algebraic computations provide the derivatives of r with respect to the Delaunay's variables.

2.2 The planar, circular problem: a truncated Hamiltonian function

Let us rewrite the perturbing function (3) as

$$R(L, G, \ell, g) = r \cos(\varphi - \psi) - \frac{1}{\sqrt{1 + r^2 - 2r \cos(\varphi - \psi)}} ;$$

we can expand the second term of R using the Legendre's polynomials P_j as (see [3])

$$\frac{1}{\sqrt{1 + r^2 - 2r \cos(\varphi - \psi)}} = \sum_{j=0}^{\infty} P_j(\cos(\varphi - \psi)) r^j .$$

The Legendre polynomials are recursively defined by

$$\begin{aligned} P_0(x) &= 1 , \\ P_1(x) &= x , \\ P_{j+1}(x) &= \frac{(2j+1)P_j(x)x - jP_{j-1}(x)}{j+1} \quad \forall j \geq 1 . \end{aligned}$$

Henceforth, R can be expanded as

$$R = -1 - \sum_{j=2}^{\infty} P_j(\cos(\varphi - \psi)) r^j .$$

The quantities φ and r are expressed in terms of the Delaunay's variables, using (4), (5), (6). This procedure leads to the Fourier development of the perturbing function, which can be written as

$$R(L, G, \ell, g) = \sum_{m, n \in \mathbf{Z}} R_{mn}(L, G) \cos(m\ell + ng) , \quad (8)$$

where $R_{mn}(L, G)$ denote the Fourier coefficients. In [2] a *truncated* model has been introduced by considering a finite Fourier development of the perturbing function, so to have a trigonometric series (namely, with a finite number of Fourier coefficients). The order of the truncation of the Fourier development depends upon the physical and orbital parameters of the interacting bodies. In [2] the asteroids Iris, Victoria and Renzia have been considered and we intend to study in the present work the dynamical stability of the same objects.

We briefly recall the criterion adopted in [2] for the truncation of the perturbing function. The planar, circular, restricted three-body model is constructed on the basis of several simplifying assumptions. Among the neglected contributions, the most significative ones (in the case of Iris, Victoria and Renzia) are the following: the eccentricity of Jupiter's orbit, the relative inclination of the asteroid and of Jupiter orbits, the gravitational influence of Mars and Saturn. Since we have neglected these effects, we shall consistently drop in the series expansion of R all those Fourier terms, whose size is of the same order of magnitude or less than the neglected contributions. For the asteroids Iris, Victoria and Renzia, this criterion leads to the definition of a *truncated* model as described by the Hamiltonian function

$$H(L, G, \ell, g) = -\frac{1}{2L^2} - G + \varepsilon R(L, G, \ell, g), \quad (9)$$

where

$$\begin{aligned} R(L, G, \ell, g) &= -1 - \frac{L^4}{4} \left(1 + \frac{9}{16}L^4 + \frac{3}{2}e^2\right) + \frac{L^4 e}{2} \left(1 + \frac{9}{8}L^4\right) \cos \ell - \frac{3}{8}L^6 \left(1 + \frac{5}{8}L^4\right) \cos(\ell + g) \\ &+ \frac{L^4 e}{4} (9 + 5L^4) \cos(\ell + 2g) - \frac{L^4}{4} \left(3 + \frac{5}{4}L^4\right) \cos(2\ell + 2g) - \frac{3}{4}L^4 e \cos(3\ell + 2g) \\ &- \frac{5}{8}L^6 \left(1 + \frac{7}{16}L^4\right) \cos(3\ell + 3g) - \frac{35}{64}L^8 \cos(4\ell + 4g) - \frac{63}{128}L^{10} \cos(5\ell + 5g). \end{aligned}$$

We remark that the above Hamiltonian function is expressed in terms of two degrees of freedom; therefore, the dimension of the phase space is 4, the constant energy surfaces have dimension 3, while invariant tori are 3-dimensional. As a consequence, invariant tori separate the constant energy surfaces, providing a strong stability property, in the sense of confinement in the phase space. The unperturbed frequency (i.e., when $\varepsilon = 0$) is given by the vector $(\omega_1, \omega_2) = (\Omega, -1)$ with $\Omega = \frac{1}{L^3}$; we shall be interested to compute the modulus of the ratio of the frequency's components, $|\frac{\omega_1}{\omega_2}| = |\frac{1}{L^3}|$.

We consider also a *reduced* model in which we further neglect the last three Fourier components. This procedure gives us a measure of the *weight* associated to different Fourier terms. In this perspective, we consider (9) with R given by

$$\begin{aligned} R(L, G, \ell, g) &= -1 - \frac{L^4}{4} \left(1 + \frac{9}{16}L^4 + \frac{3}{2}e^2\right) + \frac{L^4 e}{2} \left(1 + \frac{9}{8}L^4\right) \cos \ell - \frac{3}{8}L^6 \left(1 + \frac{5}{8}L^4\right) \cos(\ell + g) \\ &+ \frac{L^4 e}{4} (9 + 5L^4) \cos(\ell + 2g) - \frac{L^4}{4} \left(3 + \frac{5}{4}L^4\right) \cos(2\ell + 2g) - \frac{3}{4}L^4 e \cos(3\ell + 2g). \end{aligned}$$

2.3 The planar, elliptic, truncated problem

In the present section we assume that P_2 orbits around P_0 on an elliptic orbit with eccentricity equal to $e' = 0.0482$ (i.e. the eccentricity of Jupiter). In this case, we cannot perform anymore

the change of variables (1). The motion is described by a Hamiltonian function with three degrees of freedom; therefore, invariant tori do not provide the stability through confinement of the phase space: in fact, the dimension of the phase space is 6, the constant energy level surfaces have dimension 5 and consequently the 3-dimensional invariant tori do not separate the phase space. Using the same criterion adopted in section 2.2, we retain only the most significant Fourier terms in the series development of the perturbing function. The corresponding Hamiltonian takes the form:

$$H(L, G, \Psi, \ell, g, \psi) = -\frac{1}{2L^2} + \Psi + \varepsilon R(L, G, \ell, g, \psi) ,$$

where $R(L, G, \ell, g, \psi)$ depends also on e' and it is given by

$$\begin{aligned} R(L, G, \ell, g, \psi) = & -1 - \frac{L^4}{4} \left(\frac{5}{2} + \frac{9}{16} L^4 - \frac{3}{2} \frac{G^2}{L^2} + \frac{3}{2} e'^2 \right) + L^4 \frac{e}{2} \left(1 + \frac{9}{8} L^4 \right) \cos(\ell) \\ & - \frac{3}{8} L^6 \left(1 + \frac{5}{8} L^4 \right) \cos(\ell + g - \psi) + \frac{L^4}{4} e (9 + 5L^4) \cos(\ell + 2g - 2\psi) \\ & - \frac{L^4}{4} \left(3 + \frac{5}{4} L^4 \right) \cos(2\ell + 2g - 2\psi) - \frac{3}{4} L^4 e \cos(3\ell + 2g - 2\psi) \\ & - \frac{5}{8} L^6 \left(1 + \frac{7}{16} L^4 \right) \cos(3\ell + 3g - 3\psi) - \frac{35}{64} L^8 \cos(4\ell + 4g - 4\psi) \\ & - \frac{63}{128} L^{10} \cos(5\ell + 5g - 5\psi) - L^4 \left(\frac{3}{4} e' + \frac{45}{64} L^4 e' \right) \cos(\psi) \\ & - L^4 \left(\frac{21}{8} e' + \frac{45}{32} e' L^4 \right) \cos(2\ell + 2g - 3\psi) \\ & - L^4 \left(-\frac{3}{8} e' + \frac{5}{32} e' L^4 \right) \cos(2\ell + 2g - \psi) . \end{aligned}$$

2.4 The circular, inclined, truncated problem

In this section we consider the motion of P_2 around P_0 as circular, but we assume that the relative inclination i between the planes of the orbits of P_1 and P_2 is different from zero.

According to [3] we introduce a new pair of conjugated variables defined as (H, h) , where $H = G \cos i$ and h is the longitude of the ascending node. One easily finds that the Hamiltonian function depends on the difference $h - \psi$. Therefore, we perform the symplectic change of coordinates:

$$\begin{aligned} \ell &= \ell & L &= L \\ g &= g & G &= G \\ p &= h - \psi & P &= H , \end{aligned}$$

with (P, p) being conjugated variables. In terms of these quantities, we write the Hamiltonian function as

$$H(L, G, P, \ell, g, p) = -\frac{1}{2L^2} - P + \varepsilon R(L, G, P, \ell, g, p) ,$$

where, denoting by $\gamma = \sqrt{\frac{1}{2} - \frac{P}{2G}}$, one has

$$R(L, G, P, \ell, g, p) = -1 - L^4 \left(\frac{1}{4} + \frac{3}{8} e^2 + \frac{9}{64} L^4 - \frac{3}{2} \gamma^2 \right)$$

$$\begin{aligned}
& -\left(\frac{3}{4} - \frac{3}{2}\gamma^2 + \frac{5}{16}L^4\right) \cos(2\ell + 2g + 2p) \\
& -\left(-\frac{1}{2}e + 3\gamma^2e - \frac{9}{16}eL^4\right) \cos(\ell) - \left(\frac{3}{4}e - \frac{3}{2}\gamma^2e\right) \cos(3\ell + 2g + 2p) \\
& -\left(-\frac{9}{4}e + \frac{9}{2}\gamma^2e - \frac{5}{4}eL^4\right) \cos(\ell + 2g + 2p) - \frac{3}{2}\gamma^2 \cos(2\ell + 2g) \\
& -\frac{3}{2}\gamma^2 \cos(2p) - \frac{3}{2}\gamma^2e \cos(3\ell + 2g) + \frac{9}{2}\gamma^2e \cos(\ell + 2g) + \frac{3}{2}\gamma^2e \cos(\ell + 2p) \\
& + \frac{3}{2}\gamma^2e \cos(\ell - 2p) - L^6\left(\frac{3}{8} + \frac{15}{64}L^4\right) \cos(\ell + g + p) \\
& -\left(\frac{5}{8} + \frac{35}{128}L^4\right)L^6 \cos(3\ell + 3g + 3p) \\
& -\frac{35}{64}L^8 \cos(4\ell + 4g + 4p) - \frac{63}{128}L^{10} \cos(5\ell + 5g + 5p) .
\end{aligned}$$

Since the phase space has dimension 6, the separation into invariant tori is not possible also in the present case.

3 The frequency analysis

The determination of the fundamental frequencies can be obtained through frequency analysis, following the well-known standard method introduced by J. Laskar ([7], [8] to which we refer for details). For a two-dimensional Hamiltonian system, frequency analysis allows to compute the two fundamental frequencies. Roughly speaking, we study the behaviour of the so-called *frequency-map*, provided by the variation of the absolute value of the ratio of the two main frequencies as a function of the initial value of one action variable (the initial angles can be set to zero).

From the frequency map, we can infer some properties concerning the stability of the dynamics. In particular, let us consider an object with fixed frequency (ω_1, ω_2) ; we shall see that its stability is strictly related to the behaviour of the dynamics in a suitable interval around the ratio $|\frac{\omega_1}{\omega_2}|$.

To be concrete, in the case of the planar, circular, restricted three-body problem, we proceed as follows. Let us call the fundamental frequencies (ω_L, ω_G) and let $\gamma \equiv |\frac{\omega_L}{\omega_G}|$. Let L_0 be the initial value of L ; we compute the ratio $\gamma \equiv |\frac{\omega_L}{\omega_G}|$ and we vary L_0 by looking at the graph of the frequencies' ratio versus L_0 . In order to characterize regular and chaotic regimes, we follow the criterion introduced in [7], [8] (see also [9]):

a) If the curve is *regular* in a neighbourhood of γ (i.e., monotonically increasing or decreasing), then we expect to find a region of invariant tori. We remark that this criterion is valid for slightly perturbed Hamiltonian systems. For example, let us consider the planar-circular problem; then, up to terms of order ε one finds $\gamma = |1/L^3|$. Therefore, the monotone behaviour of γ is preserved at least for low values of the perturbing parameter. In particular, the frequency ratio is monotone within a large portion of the phase space, where KAM tori still survive.

b) A *resonant regime* is characterized by a straight line, showing no variation of the frequencies' ratio on a significant region of the graph. To clarify this criterion, let us consider the analogy

with the librational regime of the pendulum: when computing the frequencies in the librational region of the phase space, one finds that all frequencies are the same (in particular, they are equal to zero). The same phenomenon appears in resonant zones of more general systems.

c) A *chaotic region* is described by consecutive sudden jumps of the frequencies' ratio. Actually, the frequencies are defined only for regular curves; when entering a chaotic region, the numerical algorithm provides values of the frequencies which significantly change from one orbit to a nearby trajectory (the computed value of the frequency might also change with time on the same orbit). This phenomenon gives rise to large variation patterns of the frequency map.

When dealing with the planar, circular, restricted three-body problem (either with the full or truncated Hamiltonian), we implement frequency analysis according to the following procedure. Fix a level energy $E = E_0$ and a value $\varepsilon = \varepsilon_0$ for the perturbing parameter. Set the initial data as $L = L_0$, $\ell = 0$, $g = 0$ (the value of L_0 can be chosen arbitrarily). In order to find $G = G_0$, we solve the equation

$$E_0 = -\frac{1}{2L_0^2} - G + \varepsilon_0 R(L_0, G, 0, 0) ,$$

implementing a Newton method. We integrate the equations of motion by a IV order Runge–Kutta method with fixed step–size and we compute the main frequencies (ω_L, ω_G) by implementing frequency analysis on the set of data $(L(t_k) + \ell(t_k), G(t_k) + g(t_k))$ ¹, where $t_k = 0.1 \cdot k$ is the integration time. Finally, we compute the ratio $|\frac{\omega_L}{\omega_G}|$ that we plot as a function of L_0 for different values of L_0 with step–size $2 \cdot 10^{-5}$.

In the case of the planar, elliptic, restricted three-body problem, we fix again $E = E_0$, $\varepsilon = \varepsilon_0$ and we set the initial values as $\ell_0 = g_0 = t_0 = 0$, $L = L_0$, $G = G_0$. Here L_0 is arbitrary, G_0 is calculated as in the circular problem, while the value $\Psi = \Psi_0$ is computed in order to preserve the energy as

$$\Psi = E + \frac{1}{2L_0^2} - \varepsilon_0 R(L_0, G_0, 0, 0, 0) .$$

Frequency analysis is performed over the set of data $(L(t_k) + \Psi(t_k) + \ell(t_k), G(t_k) + g(t_k) + \psi(t_k))$, where $t_k = 0.1 \cdot k$ is the integration time. Finally, we compute the ratio $|\frac{\omega_L}{\omega_G - \omega_\Psi}|$, which is plotted versus L_0 for different values of L_0 with step–size $2 \cdot 10^{-5}$.

For the circular, inclined, restricted three-body problem, we fix $\varepsilon = \varepsilon_0$, the energy level $E = E_0$ and the initial values as $\ell_0 = g_0 = p_0 = 0$, $L = L_0$, $G = G_0$, where L_0 is arbitrary and G_0 is computed as for the planar, circular problem. If i denotes the relative inclination of the orbits, the initial value of $P = P_0$ is defined as $P_0 = G_0 \cos i$. Frequency analysis is implemented using the set of data provided by $(L(t_k) + \ell(t_k) + P(t_k), G(t_k) + g(t_k) + p(t_k))$, where $t_k = 0.1 \cdot k$ is the integration time. We compute the ratio $|\frac{\omega_L}{\omega_G + \omega_P}|$, plotted versus L_0 for different L_0 's with step–size $2 \cdot 10^{-5}$.

¹Numerical experiments show that the best result is achieved when the signal is obtained by *mixing* action and angle variables.

Table 1:

Asteroid	a_A (AU)	e	i (deg)
Iris	2.386	0.230	5.524
Victoria	2.335	0.220	8.363
Renzia	2.263	0.294	1.882

4 Stability of asteroids and of nearby invariant tori

We consider the motion of three bodies in the framework of one of the models described in section 2, where we identify P_0 with the Sun, P_1 with an asteroid and P_2 with Jupiter. In particular, we are interested in studying the dynamics of the asteroids Iris, Victoria and Renzia. Their elliptic elements (see [12]) are listed in Table 1: a_A represents the major semiaxis in Astronomical Units AU ($1 AU = 150 \cdot 10^6 km$ is the average Earth–Sun distance), e denotes the orbital eccentricity and i is the inclination (measured in degrees).

We remarked that the stability property, in the sense of confinement in phase space, can be obtained only in the two–dimensional case of the planar, circular, restricted three–body problem. In this context, invariant tori provide a separation on the constant energy surfaces. The idea developed in [2] is to fix a level of energy and to prove the existence of two invariant tori bounding, from above and below, the motion of the asteroid. We shortly recall such procedure referring to [2] for the complete details.

Let $m_S = 1.991 \cdot 10^{30} kg$ and $m_J = 1.9 \cdot 10^{27} kg$ be the observed masses of the Sun and Jupiter, respectively. Define $m_2 = \frac{m_J}{m_S + m_J}$, $m_0 = 1 - m_2$, $\mu = \frac{1}{m_0^{2/3}}$; then, let $L_{obs} = \mu \sqrt{m_0 a}$ and $G_{obs} = L_{obs} \sqrt{1 - e^2}$, where a is the major semiaxis in normalized Jupiter–Sun distance, i.e. $a = \frac{a_A}{a_J}$, where $a_J = 5.203 AU$. The quantities a_A and e are given in Table 1. Let $\omega_{obs} = \frac{1}{L_{obs}^3}$ be the *observed* frequency of the asteroid. The energy level is chosen as the *unperturbed* energy (i.e., taking $\varepsilon = 0$) of the asteroid: $E_{obs} = -\frac{1}{2L_{obs}^2} - G_{obs}$. Moreover, let $\tilde{L}_\pm = L_{obs} \pm 0.001$ and define $\tilde{\omega}_\pm = \frac{1}{\tilde{L}_\pm^3}$. Compute the continued fraction representation up to the order 5 of the frequencies $\tilde{\omega}_\pm$:

$$\tilde{\omega}_\pm = [a_1; a_2, a_3, a_4, a_5, \dots] = a_1 + \frac{1}{a_2 + \frac{1}{a_3 + \frac{1}{a_4 + \frac{1}{a_5 + \dots}}}} .$$

Modify $\tilde{\omega}_\pm$ by adding a tail of one’s after the 5th term of the continued fraction expansion; in this way, one obtains irrational numbers $\omega_\pm = [a_1; a_2, a_3, a_4, a_5, 1^\infty]$, satisfying the so–called *diophantine condition*:

$$|\omega_\pm - \frac{p}{q}|^{-1} \leq C_\pm |q|^2 , \quad \forall p, q \in \mathbf{Z} , q \neq 0 , \quad (10)$$

for some positive real constants C_\pm which can be evaluated by number theory (see [2]). Finally, let $L_\pm = \frac{1}{\omega_\pm^{1/3}}$ and $G_\pm = -\frac{1}{2L_\pm^2} - E_{obs}$, where the eccentricity is provided by $e_\pm = \sqrt{1 - (\frac{G_\pm}{L_\pm})^2}$. We fix the energy level of the asteroid by selecting $E = E_{obs} + \varepsilon \bar{R}(L_{obs}, G_{obs})$,

Table 2:

Asteroid	E_{obs}	ω_{obs}	ω_-	ω_+
Iris	-1.749108	3.220143	3.204407	3.232969
Victoria	-1.767380	3.326216	3.309769	3.339560
Renzia	-1.779669	3.486213	3.460913	3.508431

where $\bar{R}(L_{obs}, G_{obs})$ is the average over the angle variables of the perturbing function related to the truncated model presented in section 2.2:

$$\bar{R}(L_{obs}, G_{obs}) = -1 - \frac{L_{obs}^4}{4} \left(1 + \frac{9}{16} L_{obs}^4 + \frac{3}{2} e_{obs}^2 \right),$$

where $e_{obs} = \sqrt{1 - \frac{G_{obs}^2}{L_{obs}^2}}$. We report in Table 2 the values of the unperturbed energy level, of the observed frequency ω_{obs} and of the frequencies of the bounding tori, ω_- and ω_+ (using proper units).

The existence of the bounding tori with frequencies $(\omega_-, -1)$ and $(\omega_+, -1)$ has been obtained in [2] by applying a computer-assisted isoenergetic KAM theorem. Such theory can be applied under quite general assumptions; a necessary requirement is that the frequency satisfies the diophantine condition (10). The existence of invariant surfaces is proven for values of $\varepsilon \leq 0.001$, showing a full agreement between the theoretical result and the realistic physical value corresponding to the Jupiter-Sun mass-ratio. We refer to [2] for an exhaustive explanation of the results.

In order to provide a numerical investigation of the model adopted in [2], we apply frequency analysis to compute the break-down value of the tori with frequencies $(\omega_-, -1)$ and $(\omega_+, -1)$. We recall that when the confinement property holds, the existence of such tori implies the stability of the asteroid; on the contrary, if one of the two tori ceases to exist, one cannot infer instability of the motion of the minor body: for example, there could still exist bounding tori with different frequencies.

We apply the frequency analysis with a twofold aim:

- 1) to determine the break-down value of the tori with frequencies $(\omega_-, -1)$ and $(\omega_+, -1)$,
- 2) to provide numerical evidence of the stability of the asteroid, whenever the confinement property applies.

Let us denote by ε_c the critical value of the perturbing parameter at which the transition from stability to instability occurs. We present the results in the following form (see Tables 3, 4, 5; compare also with Figures 1, 2, 3):

i) we provide an interval, say $\varepsilon_- < \varepsilon_c \leq \varepsilon_+$, such that if $\varepsilon_c \leq \varepsilon_-$, then both lower and upper bounding tori exist, while if $\varepsilon_c \geq \varepsilon_+$ both tori have disappeared. This means that in the case of the planar, circular, restricted three-body problem, for $\varepsilon_c \leq \varepsilon_-$ the motion of the asteroid is confined on the preassigned energy level between the two bounding tori;

ii) we provide some intermediate values (denoted by "IV") at which one of the two tori still survives, while the other torus disappeared.

Table 3:

Asteroid	Complete	IV	Truncated	IV
Iris	$0.03 < \varepsilon_c \leq 0.05$	0.04	$0.06 < \varepsilon_c \leq 0.08$	0.07
Victoria	$0.03 < \varepsilon_c \leq 0.051$	0.04–0.05	$0.05 < \varepsilon_c \leq 0.08$	0.06–0.07
Renzia	$0.06 < \varepsilon_c \leq 0.08$	0.07	$0.01 < \varepsilon_c \leq 0.03$	0.02

Table 4:

Asteroid	Reduced	IV
Iris	$0.08 < \varepsilon_c \leq 0.1$	0.09
Victoria	$0.08 < \varepsilon_c \leq 0.1$	0.09
Renzia	$0.02 < \varepsilon_c \leq 0.03$	0.025

The results for the planar, circular, restricted three–body model in the framework of the complete and truncated Hamiltonians are the presented in Table 3.

We have investigated also a *reduced* truncated Hamiltonian model, in the context of the planar, circular, restricted three–body model. More precisely, in the Fourier expansion of the perturbing function, we dropped the terms related to $\cos(3\ell + 3g)$, $\cos(4\ell + 4g)$, $\cos(5\ell + 5g)$. The results are presented in Table 4.

Finally, we provide in Table 5 the results concerning the planar–elliptic and circular–inclined models.

A graphical inspection is provided by Figures 1, 2, 3. Concerning the planar, circular, restricted, three–body model, the frequency is given by a two–dimensional vector, say (ω_L, ω_G) , which is computed by frequency analysis. In Figure 1 we display the modulus of the ratio of the components $|\frac{\omega_L}{\omega_G}|$ versus the initial action variable L_0 . In Figure 1a we use the truncated Hamiltonian (see section 2.2) and we provide the results for different values of ε . We recall that in the unperturbed case, the second component of the frequency vector is -1, so that the modulus of the ratio of the two components of the frequency vector of the bounding tori coincides with ω_- or ω_+ ; to this end, the lines corresponding to the values $\Omega_- \equiv |\frac{\omega_-}{-1}|$ and $\Omega_+ \equiv |\frac{\omega_+}{-1}|$ are also displayed. We notice that for $\varepsilon = 0.05$ both tori exist, while only the upper

Table 5:

Asteroid	Elliptic	IV	Inclined	IV
Iris	$0.05 < \varepsilon_c \leq 0.07$	0.06	$0.06 < \varepsilon_c \leq 0.08$	0.07
Victoria	$0.05 < \varepsilon_c \leq 0.07$	0.06	$0.06 < \varepsilon_c \leq 0.08$	0.07
Renzia	$0.08 < \varepsilon_c \leq 0.11$	0.09–0.1	$0.09 < \varepsilon_c \leq 0.13$	0.1–0.12

torus survives for $\varepsilon = 0.06 - 0.07$ and both tori disappeared at $\varepsilon = 0.08$, since there are no orbits with values of the frequencies in the interval $[\Omega_-, \Omega_+]$. Let us remark that the abrupt interruption for larger L_0 is due to the condition of existence of G_0 . Indeed, the eccentricity is related to the action variables by $e = \sqrt{1 - G_0^2/L_0^2}$: to have a physical meaning, the eccentricity must be a real number, implying that the system must satisfy the condition that $G_0 \leq L_0$. This argument imposes an upper bound on the choice of L_0 .

We remark that this criterium of breakdown of stability is a bit different from the usual one based on the transition from a monotonic variation of the frequency map to a noisy one.

A similar analysis is performed in the case of the reduced Hamiltonian (see section 2.2), which contains a minor number of Fourier terms than in the case of the truncated Hamiltonian. The results are presented in Figure 1b for $\varepsilon = 0.08, 0.09, 0.1$.

Let us consider now the complete Hamiltonian (see section 2.1). For the actual value of the Jupiter–Sun mass–ratio, the results concerning the truncated and complete Hamiltonians show the same dynamical features. As far as the strength of the perturbation is increased, the two models differ consistently. Indeed, Figure 2 shows the results of the frequency analysis for $\varepsilon = 0.03, 0.04$ and 0.051 . The motion seems to be regular for $\varepsilon = 0.03$ and both tori with frequencies $(\omega_-, -1)$ and $(\omega_+, -1)$ survive the perturbation. On the contrary, for $\varepsilon = 0.04$ only one torus survives, while for $\varepsilon = 0.051$ both tori disappeared.

As shown in Figure 3, the truncated model still preserves a regular character, even when the effects of the eccentricity of Jupiter or of the mutual inclination are considered. In particular, Figure 3a concerns the planar, elliptic, restricted model; in order to compare the results with those obtained for the truncated model, we plotted the quantity $|\frac{\omega_L}{\omega_G - \omega_\Psi}|$ versus L_0 . The results for the (truncated) inclined model are displayed in Figure 3b, where the quantity $|\frac{\omega_L}{\omega_G + \omega_P}|$ is plotted versus L_0 .

5 Conclusions

The Fourier analysis performed in the previous section allows to draw the following conclusions.

i) We compute an approximation of the critical break–down value of the invariant surfaces with frequencies $(\omega_-, -1)$ and $(\omega_+, -1)$, to be compared with the analytical results obtained in [2]. We remark that one could apply alternative numerical methods for the determination of the transition value; however, the actual techniques are often adapted to very simple mathematical problems and they do not provide reliable results for more sophisticated models, like the one studied in the present work.

ii) In the context of the planar, circular, restricted three–body problem, the existence of the bounding tori guarantees the confinement of the asteroid; therefore, we can interpret the results shown in Table 3 as a lower bound on the stability of the minor body. For example, there is numerical evidence of the stability of Iris and Victoria for any mass–ratio $\varepsilon \leq 0.03$, when using the complete expression of the perturbing function. When adopting the truncated model, the frequency analysis suggests that Iris is stable for any $\varepsilon \leq 0.06$ and Victoria is stable for any

$\varepsilon \leq 0.05$.

iii) The frequency analysis provides a tool for comparing the different models described in section 2. More precisely, we start by evaluating the difference between the complete and truncated Hamiltonians. The critical values are different by a factor about equal to 2; however, the astronomical value of the Jupiter–Sun mass–ratio ($\varepsilon \simeq 10^{-3}$) is well below the critical estimates reported in Table 3.

Focussing on the truncated Hamiltonian, we test its validity by lessening the number of Fourier terms retained in the series development of the perturbing function. A comparison between Tables 3 and 4 shows that a minor number of Fourier terms is still sufficient to compute the critical break–down values with good accuracy.

Finally, in order to evaluate the effect of the eccentricity of Jupiter and of the inclination of the orbits, we performed the Fourier analysis on the models described in section 2.3 and 2.4. In the cases of Iris and Victoria, the results presented in Table 5 do not differ significantly from the values reported in Table 3 for the planar–circular truncated case, thus providing a further validation of the efficacy of the truncated model. A more evident discrepancy is found when we investigate the asteroid Renzia, due to the fact that its frequency is close to a $7/2$ resonance.

We believe that the strategy proposed in this paper can be conveniently applied to a wide set of asteroids, providing useful information about the dynamics of minor bodies. We plan to continue along these lines in a future work.

Acknowledgments: We thank David Nesvorny for having provided in public domain a software for computing the frequencies by means of the Laskar’s method. We are grateful to L. Chierchia for critically reading the manuscript.

References

- [1] Arnold V.I.: *Proof of a Theorem by A.N. Kolmogorov on the invariance of quasi-periodic motions under small perturbations of the Hamiltonian*, Russian Math. Survey **18**, 9 (1963)
- [2] Celletti A., Chierchia L.: *KAM Stability and Celestial Mechanics*, Preprint (2003)
- [3] Delaunay C.: *Théorie du Mouvement de la Lune*, Mémoires de l’Académie des Sciences **1**, Tome XXVIII, Paris (1860)
- [4] Hénon M.: *Explorations numérique du problème restreint IV: Masses égales, orbites non périodique*, Bulletin Astronomique **3**, no. 1, fasc. 2, 49-66 (1966)
- [5] Kolmogorov A.N.: *On the conservation of conditionally periodic motions under small perturbation of the Hamiltonian*, Dokl. Akad. Nauk. SSR **98**, 469 (1954)
- [6] Kovalevsky J.: *Introduction à la Mécanique Céleste*, Librairie Armand Colin, Paris (1963)
- [7] Laskar J., Froeschlé C., Celletti A.: *The measure of chaos by the numerical analysis of the fundamental frequencies. Application to the standard mapping*, Physica D, **56**, 253 (1992)

- [8] Laskar J.: *Frequency analysis for multi-dimensional systems. Global dynamics and diffusion*, Physica D, **67**, 257 (1993)
- [9] Lega E., Froeschlé C.: *Numerical investigation of the structure around an invariant KAM torus using the frequency map analysis*, Physica D, **95**, 97 (1996)
- [10] Moser J.: *On invariant curves of area-preserving mappings of an annulus*, Nach. Akad. Wiss. Göttingen, Math. Phys. Kl. II **1**, 1 (1962)
- [11] Roy A.E.: *Orbital Motion*, Adam Hilger Ltd., Bristol (1978)
- [12] Small-Body Orbital Elements: http://ssd.jpl.nasa.gov/sb_elem.html

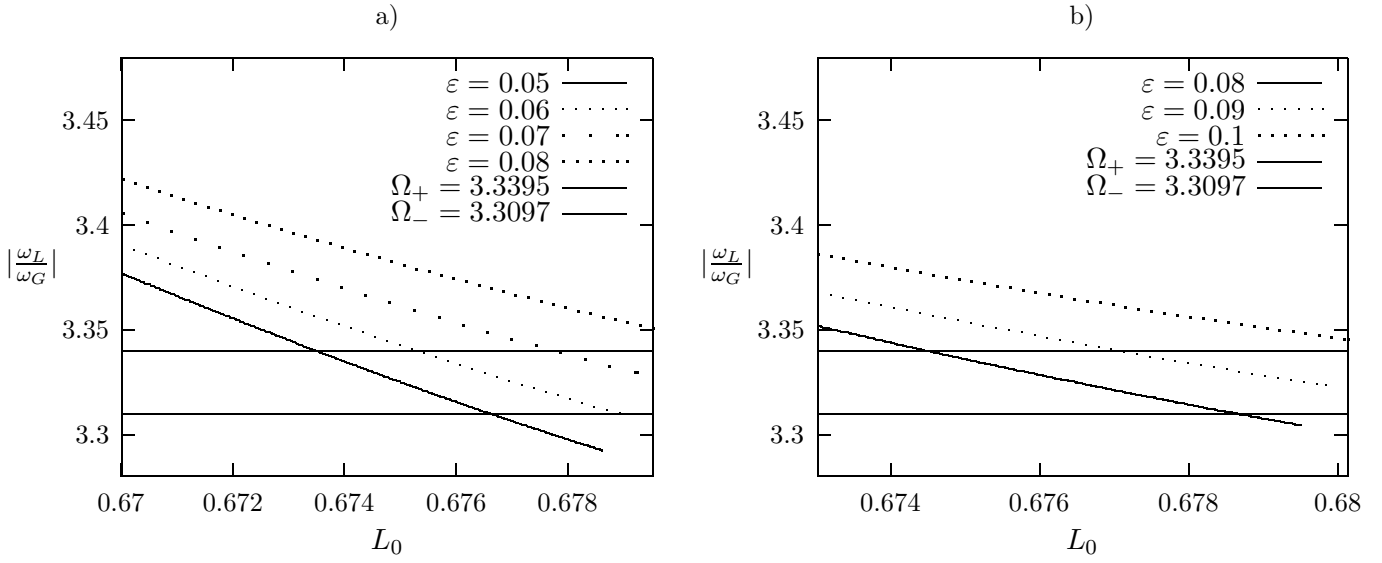


Figure 1: Results of the frequency analysis for the asteroid Victoria in the framework of the planar, circular, restricted, three-body model: a) truncated Hamiltonian, b) reduced Hamiltonian.

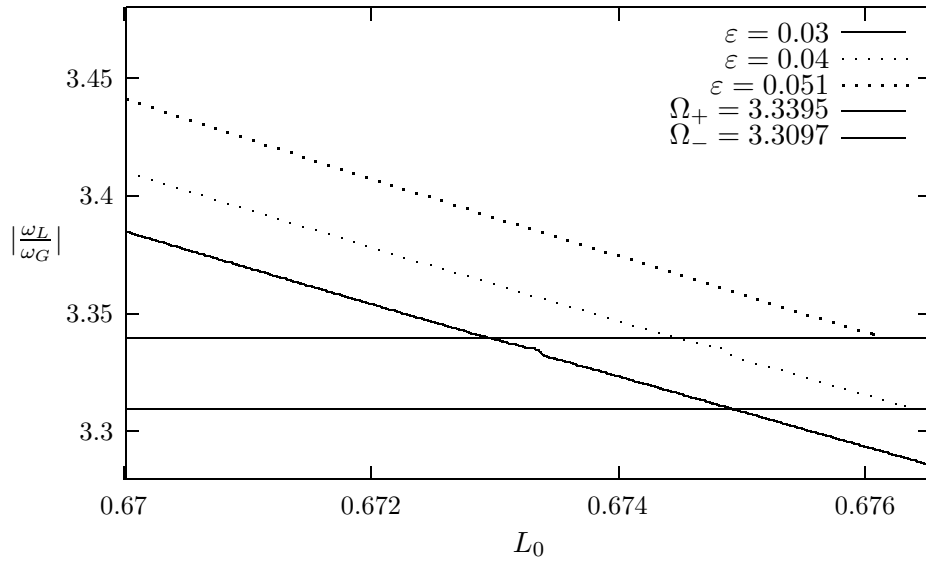


Figure 2: Results of the frequency analysis for the asteroid Victoria in the framework of the planar, circular, restricted, three-body model, using the complete Hamiltonian function.

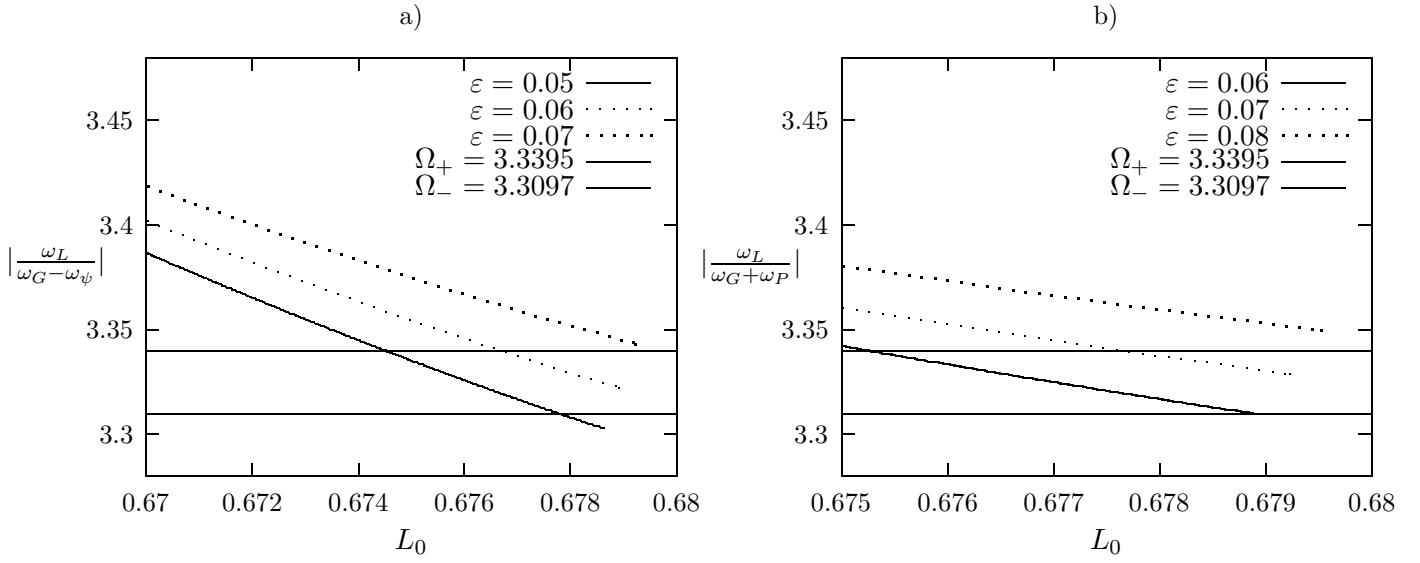


Figure 3: Results of the frequency analysis for the asteroid Victoria in two different settings: *a)* the planar, elliptic, restricted, three-body model, *b)* the inclined, circular, restricted, three-body model.